Online ISSN 1848-3380, Print ISSN 0005-1144
ATKAFF 57(3), 793–809(2016)

Farzad H. Panahi, Parvin Farhadi and Zhila H. Panahi

Spectral-Efficient Green Wireless Communications via Cognitive UWB Signal Model

DOI 10.7305/automatika.2017.02.910
UDK 621.396.018.424.029.63.091.1:681.5.015.87-047.58

Original scientific paper

This paper focuses on spectral lines suppression for non-coherent impulse-radio ultra-wideband (IR-UWB) signals in the presence of pulse attenuation and timing jitter. Particular attention is devoted to severely unbalanced (i.e. non-uniform distributed) data sources where a unified spectral analysis is considered for both uncorrelated and correlated M-ary biorthogonal data-stream scenarios. Indeed, the specific novelty insights of this paper are as follows: i) Proposal of a new spectral-efficient signal model as a modified version of transmitted-reference (TR) approach, where each transmitted symbol is represented by a preamble Data-based Statistical Reference (DSR) followed by a set of transmitted data pulses and within this context, the preamble signal is designed to eliminate spectral lines via an adaptive monitoring of data-stream statistics as the optimal spectral policy; ii) Performance analysis in order to derive optimal signal parameters; iii) Evaluation of the system capabilities over different predefined operational modes.

Key words: Spectral-Efficient Green Wireless Communications, Optimal Spectral Policy, Cognitive UWB Signal Model

Spektralno-efikasna zelena bežična komunikacija pomoću kognitivnog UWB signalnog modela. Ovaj rad se fokusira na prigušenje spektralnih linija kod ne-koherentnih radio-impulsnih ultra-širokopojasnih (IR-UWB) signala prilikom slabljenja pulsa i vremenskog podrhtavanja. Posebna pažnja je pridana značajno neuravnoteženim (npr. ne-uniformnmno distribuiranim) izvorima podataka gdje je jedinstvena spektralna analiza razmatrana za nekorelirane i korelirane M-arne biortogonalne scenarije prijenosa podataka. Novine predstavljene u ovom radu su: i) Novi spektralno-efikasni signalni model koji je modificirana verzija pristupa prijenosom-reference (TR), gdje se svaki preneseni simbol prikazuje pomoću preambule definirane statistikom reference podataka (DSR) koju slijedi skup prenesenih podatkovnih pulseva, te je u tom kontekstu preambula signala dizajnirana kako bi se eliminirale spektralne linije pomoću optimalnog spektralnog kriterija definiranog adaptivnim praćenjem statistike poslanih podataka; ii) Analiza performansi kako bi se dobili optimalni parametri signala i iii) Evaluacija sposobnosti sustava prilikom rada u različitim predefiniranim stanjima.

Ključne riječi: Spektralno-efikasna zelena bežična komunikacija, Optimalni spektralni kriterij, Kognitivni UWB signalni model

1 INTRODUCTION

In recent years, Ultra-Wideband (UWB) spectrum shaping has attracted significant interest from researchers and engineers in the communication field. Most spectrum shaping techniques used in many researches offer strict-synchronization based solutions to overcome spectrum problems such as power spectral lines [1-5]. The undesired power spectral lines not only can violate Federal Communications Commission (FCC) spectrum mask and cause harmful interference to conventional radio services, but they can also correlate with strong Narrow-Band (NB) signals and cause interference to UWB signals [1-4] (See Fig. 1). However, because of the innate properties of the nanosecond UWB transmitted pulses, time synchronization is a major challenge and provides a rich area to study in UWB communication systems. Moreover, the strict power limitations and short pulse duration make the performance of UWB systems highly sensitive to timing errors such as jitter and drift [5]. So, considering the synchronization problems, it is essential to introduce a reliable transmission method that offers simple and rapid signal synchronization and simultaneously, keeps undesired power spectral lines in a reasonable Fluctuation Range (FR).

2 PROBLEM STATEMENT

So far, extensive research activities are concentrated on the design of proper Time-Hopping (TH) codes to suppress undesired spectral lines and to mitigate narrow-band interference (NBI) [6-9]. This aim is directed by introducing pseudo-random TH (PR-TH) codes and floating TH codes in [6] and [7], respectively. Note that, in the TH technique, transceivers need accurate timing and precise synchronization, which in multipath environments can lead to errors and added complexity [9]. In many other contributions, direct-sequence (DS) codes are also exploited to obtain appropriate frequency specifications [9,10]. All these methods multiply data symbols or pulses by a pseudo-random DS (PR-DS) code. Applying a perfect-random DS code to UWB system clears undesired spectral lines from power spectral density (PSD) of UWB signals completely. This case can be modeled by the use of long-period PR-DS codes. Similar investigations focus on spectral-efficient systems based on convolutional codes [11,12]. However, in spite of anti-spectral lines properties of pseudo-random codes described in the mentioned references, synchronization problems can easily cease code tracking at the receiver. Thus, the use of these codes for spectrum shaping purposes cannot be justifiable. In other words, long pseudo-random sequences make synchronization process more difficult, and complicate the design of equalizer schemes [8]. Furthermore, when the spreading gain is restricted and the interfering signals are very strong, the spreading gain cannot provide a desired level of suppression over joint spectral-lines and interferences [10].

Moreover, many other contributions in the open technical literature are referred to design FCC optimized UWB pulses [13-15], and therefore the undesired spectral lines are not taken into account when figuring a stream of unbalanced (i.e. non-uniform distributed) data bits. This means that the appearance of undesired spectral lines due to periodicity or unbalanced data sources and or variation of the PSD continuous part can easily violate the FCC spectrum mask.

Transmitted-Reference (TR) modulation has been envisioned since the 1920s for synchronizing spread-spectrum communications systems [16]. This technique is reintroduced into UWB communications recently for its simplicity [17], robust performance in multipath environments, and avoidance of the stringent synchronization requirements of conventional pulse-detection techniques. Indeed, TR-UWB technique uses an ultra-short reference pulse followed by the actual information or the data pulse to transmit data. These pairs of pulses are called doublets. The reference pulse and the data pulse are distorted by the same channel. At the receiver, the pulses are correlated and integrated, allowing the receiver to gather the whole channel energy. But, as an important disadvantage, we can refer to the innate periodicity of TR modulation that may intensify undesired spectral lines and increase the spectral fluctuation range. In this manuscript, the analysis, estimation, and shaping of the PSD of UWB signals with special view to system performance via a unified theoretical framework is a topic of major interest for the design of compliant UWB systems and although TR modulation may intensify spectral-lines and increase the spectral roughness due to its innate periodicity, but it is still recommended as a smart choice to face the UWB major challenges particularly for the synchronization process. Thus, in this paper a reliable DSR-based scheme as a modified version of TR-based signaling is presented in a way that optimized symmetric coefficients are applied to the consecutive reference signals in order to suppress undesired spectral-lines while self-synchronization properties of TR receiver are kept intact. So, just like TR-UWB applications, the proposed DSR-based UWB system (which is designated based on TR-UWB system) can be used in multimedia applications and in embedded devices to offer a low-power consuming wireless connectivity. It should be noted, to create low-power systems, standby mechanisms, energy effective detection and decoding algorithms are essential. Thus, DSR-based UWB systems can be exploited as low-power alternative in wireless personal area network systems (WPAN) or in localization applications. The main criterion for such systems is not an exceptionally high data rate, but low-power design that allows robust transceiver structures at a reasonable data rate.

Motivated by the above considerations and in order to overcome the evidenced restrictions, the present contribution is intended to report on our research advances along three major directions in the depicted context: i) Proposal of a spectral-efficient and reliable signal model with key factors for performance adjustment, and considering a unified and comprehensive theoretical framework for consistent spectral analysis; ii) Exploitation of the proposed spectral strategies to define an optimal spectral policy; iii) Evaluation of the system capabilities over different predefined operational modes.

3 NOMENCLATURE

The acronyms used throughout this paper are listed in Table 1 and the symbols are summarized in Table 2.

4 SIGNAL AND SYSTEM MODELS

This manuscript focuses on impulse radio (IR)-based UWB systems; hence, it can be assumed that the information is conveyed using very short time pulses with low duty cycle [2,18]. In the proposed signal model, each transmitted symbol is represented by a preamble DSR signal followed by several consecutive data pulses, as shown in Fig.

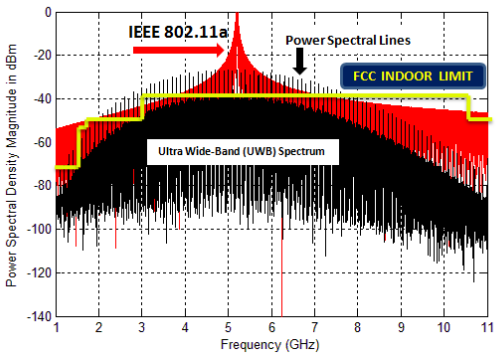

Fig. 1. Power spectral lines not only can violate FCC mask and cause harmful interference to conventional radio services, but they can also correlate with strong NB signals (e. g. IEEE 802.11a) and cause interference to UWB signals

Table 1. List of acronyms

AWGN	additive white Gaussian noise
BER	bit error rate
CF	cost function
DSR	data-based Statistical Reference
DSSS	direct sequence spread spectrum
DS-UWB	direct sequence ultra-wideband
ECC	electronic communications committee
ECMA	european computer manufacturers association
EIRP	equivalent isotropic radiated power
ETSI	european telecommunications standards institute
FCC	federal communications commission
FHSS	frequency-hopping spread spectrum
FR	fluctuation range
FSSM	moore finite-state sequential machine
MA	multiple access
MBOM	M-ary biorthogonal modulation
MC	markov chain
NBI	narrowband interference
PAM	pulse-amplitude modulation
POE	probability of error
PPM	pulse-position modulation
PRDS	pseudo random direct sequence
PRTH	pseudo random time hopping
PSD	power spectral density
SIR	signal-to-interference ratio
SNR	signal-to-noise ratio
TH	time hopping
TR	transmitted reference
UWB	ultra-wideband
WLAN	wireless local area network
WPAN	wireless personal area network

Table 2. List of Symbols

$v(t)$	Transmitted signal at time t
$g(t)$	Basic Gaussian pulse with duration T_p
$E[.]$	Expectation operator
$\{Z_n\}$	DSR sequence over the set $\{-A, A\}$
Z_d	Coefficient of data-bits
(I_n, θ_n)	n-th pair of MBOM data-bits
N_w	Number of pulses used per data symbol
T_B	Nominal shift according to θ_n
D	Time delay between DSR and data parts
T_c	Nominal shift caused by the TH sequence
T_r	Mean repetition time between pulses
$\{T_S$	Data symbol time
$\{a_{n,k}\}$	PR-DS sequence with period X_a
$\{c_{n,k}\}$	PR-TH sequence with period X_c
$\Delta_{n,k}$	Uniformly distributed random jitter
$\xi_{n,k}$	Pulse attenuation
$G(f)$	Fourier transform of $g(t)$

(2), depending upon the modulation scheme employed. Note that to perform data detection correctly, one way is to design a traceable DSR sequence under the stationary data-stream assumption. Generally, as in this paper, the signal model is considered for both uncorrelated and correlated M-ary biorthogonal data modulations. The preamble DSR signal is designed to eliminate spectral lines appeared mainly by existing unbalanced data sources. Once modulation is performed, each pulse can be subjected to additional time shifting as ruled by a PR-TH sequence, which is commonly used for multiple access (MA) purposes. Additionally, each pulse can be multiplied by a PR-DS, which can be used for MA or spreading purposes. Although each data pulse is ideally transmitted with fixed amplitude and at specific time intervals, imperfections such as jitter or attenuation should be considered in the model.

So, a reliable signal model covering the parameters previously mentioned is proposed as Eq. (1), where $v\,(t)$ is the transmitted signal at time t, $g(t)$ is the basic Gaussian pulse with duration T_p, Z_n is the n-th DSR bit (E$[Z_n]$ = μ_z, E$[Z_n Z_n^*] = \sigma_z^2 + \mu_z^2$, where $E[.]$ is the expectation operator) over the set $\{-A, A\}$ and extracts from a long periodic set with period X_z, Z_d is the coefficient of data-bits, I_n and θ_n (E$[I_n] = \mu_i$, E$[I_n I_n^*] = \sigma_i^2 + \mu_i^2$) are the n-th pair of data bits in order to construct M-ary biorthogonal data modulation. Also, N_w is the number of pulses used per data symbol ($N_w \geq 2$), T_B is the nominal shift according to θ_n, D is a constant value to make a time delay between DSR and data parts, T_r is the mean repetition time between pulses, T_s is the data symbol time ($T_s = N_w T_r + D$), $\{a_{n,k}\}$ is a PR-DS sequence with period X_a, $\{c_{n,k}\}$ is a PR-TH sequence with period X_c, T_c is the nominal shift caused by the TH sequence and $\Delta_{n,k}$, $\xi_{n,k}$ (E$[\xi_n] = \mu_\xi$, E$[\xi_n \xi_n^*] = \sigma_\xi^2 + \mu_\xi^2$) are the random jitter and attenuation, respectively. Associated with each signaling pulse is a random timing jitter, Δ, which is uniformly distributed in the interval $(-\tau_d, \tau_d)$. Without loss of generality, to avoid syn-

chronization problems, we may assume $X_z >> X_a = X_c = T_s$. It is also assumed that Z_n, I_n, θ_n, $\xi_{n,k}$, $a_{n,k}$, and $c_{n,k}$ are mutually independent of each other.

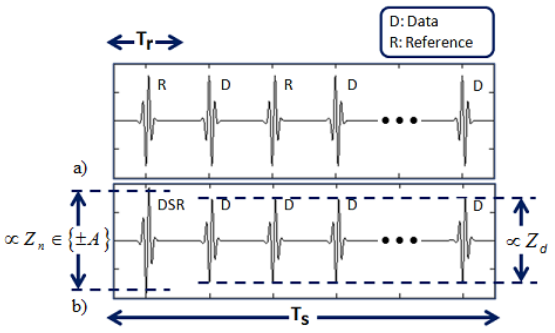

Fig. 2. Signal models: a) Conventional TR-based model. b) Spectral-efficient DSR-based model.

The spectral analysis presented in this paper for correlated unbalanced or balanced data sources is based on the state-transition diagram model, which can be interpreted as a Moore finite-state sequential machine (FSSM) and its corresponding Markov chain (MC) model as outlined in [11,19,20]. In other words, signal generation process can be represented by a Moore-Markov model which can be straightforwardly used for the spectral analysis of systems where the PAM and the PPM data streams, (I_n,θ_n), are correlated. In this case, the transmitted signal is modeled as (2), where, σ_n is the state process of the Moore-Markov model with N_M states, $g_{\sigma_{n,k}}(t - nT_s - kT_r)$ is the k-th state-pulse used for the transmission of the n-th data symbol, (I_n,θ_n), and generally may be different from DSR pulse shape. For the other parameters, descriptions in the previous subsection can be rewritten. As the purpose of this paper is to evaluate the PSD average statistics, it is assumed that the MC has reached steady state.

$$v(t) = \sum_{n=-\infty}^{+\infty} \left[Z_n \xi_n a_n g(t - nT_s - \Delta_n) + Z \sum_{k=1}^{N_w - 1} I_n \xi_{n,k} a_{n,k} g(t - nT_s - kT_r - c_{n,k}T_c - \theta_n T_B - \Delta_{n,k} - D) \right] \tag{1}$$

$$v(t) = \sum_{n=-\infty}^{+\infty} \left[Z_n \xi_n a_n g(t - nT_s - \Delta_n) + Z \sum_{k=1}^{N_w - 1} \xi_{n,k} a_{n,k} g_{\sigma_{n,k}}(t - nT_s - kT_r - c_{n,k}T_c - \Delta_{n,k} - D) \right] \tag{2}$$

5 SPECTRAL ANALYSIS

The classical method to evaluate the power spectrum of a random process modeled as a periodic repetition of a random frame is to consider an observation of $v(t)$ over the symmetric interval $(-T,T)$, compute the power spectrum for this truncated observation (i.e. $V_T(f)$), and then take the limit as the observation interval goes to infinity. Now let $2N + 1$ denote the number of frames in the $(-T,T)$-second observation. So, we have:

$$\Phi_v(f) = \lim_{N \to \infty} \frac{1}{(2N+1)T_s} E[|V_N(f)|^2] \tag{3}$$

where $E[.]$ is the expectation operator, and since we are dealing with an integer number of frames over the observation interval, we have replaced the T subscript on $V_T(f)$ with N to reflect this fact. The PSD expressions for correlated signals previously reported in the references cannot be used for the spectral analysis of the signal models proposed in Section (4). This is due to the introduction of variables such as attenuation and jitter and the fact that the effects of unbalanced data sources have not been investigated. The analysis presented, in this paper also focuses on M-ary biorthogonal data modulation for both independent and correlated data stream which can indeed be treated in a unified framework.

5.1 Independent Data Stream

According to the proposed signal model in Eq. (1), the Fourier transform of the $2T$-second observation of $v(t)$ can be expressed as (4), where $G(f)$ is the Fourier transform of the basic Gaussian pulse $g(t)$. Taking the squared magnitude of Eq. (4) and then performing the statistical expectation gives

$$E\left[|V_N(f)|^2\right] = |G(f)|^2 . [W_{I_{BDM}} + W_{II_{BDM}}] \tag{5}$$

where the factor $W_{I_{BDM}}$ accounts for the statistical expectation of the same indexed expressions and is evaluated as (6). Accordingly, the statistical expectation of the different indexed expressions is derived as, (7). However, since

timing jitter and attenuation are i.i.d., the following expectations can be written as,

$$E\left[\xi_k \xi_{k'}^*\right] = \begin{cases} \sigma_\xi^2 + \mu_\xi^2, & k = k'; \\ \mu_\xi^2, & k \neq k'. \end{cases},$$
$$E\left[e^{-j2\pi f(\Delta_k - \Delta_{k'})}\right] = \begin{cases} 1, & k = k'; \\ \phi_\Delta^2(f), & k \neq k'. \end{cases} \quad (8)$$

where $\phi_\Delta(f) = E\left[e^{-j2\pi f \Delta_k}\right] = \frac{1}{2\tau_d}\int_{-\tau_d}^{+\tau_d} e^{-j2\pi f \Delta_k} d\Delta_k = \frac{sin2\pi f\tau_d}{2\pi f \tau_d}$. To continue, let us define:

$$E\left[a_k a_{k'} e^{-j2\pi f\left(c_k - c_{k'}\right)}\right] = \phi_{ss}(n,k),$$
$$\phi_\theta(f) = E\left[e^{j2\pi f \theta_n T_B}\right] \quad (9)$$

$$V_N(f) = G(f) \sum_{n=-N}^{N} \left[Z_n \xi_n a_n e^{-j2\pi f(nT_s + \Delta_n)} + Z \sum_{k=1}^{N_w - 1} I_n \xi_{n,k} a_{n,k} e^{-j2\pi f(nT_s + kT_r + c_{n,k}T_c + \theta_n T_B + \Delta_{n,k} + D)} \right] \quad (4)$$

$$W_{I_{BDM}} = \sum_{n=-N}^{N} E\left[\left(Z_n \xi_n a_n e^{-j2\pi f(nT_s + \Delta_n)} + Z I_n \sum_{k=1}^{N_w - 1} \xi_{n,k} a_{n,k} e^{-j2\pi f(nT_s + kT_r + c_{n,k}T_c + \theta_n T_B + \Delta_{n,k} + D)} \right) \right.$$
$$\left. \cdot \left(Z_n^* \, \xi_n^* \, a_n^* e^{j2\pi f(nT_s + \Delta_n)} + Z I_n^* \sum_{k=1}^{N_w - 1} \xi_{n,k}^* a_{n,k}^* e^{j2\pi f(nT_s + kT_r + c_{n,k}T_c + \theta_n T_B + \Delta_{n,k} + D)} \right) \right] \quad (6)$$

$$W_{II_{BDM}} = \sum_{\substack{n=-N \\ m \neq n}}^{N} \sum_{m=-N}^{N} E\left[\left(Z_n \xi_n a_n e^{-j2\pi f(nT_s + \Delta_n)} + Z I_n \sum_{k=1}^{N_w - 1} \xi_{n,k} a_{n,k} e^{-j2\pi f(nT_s + kT_r + c_{n,k}T_c + \theta_n T_B + \Delta_{n,k} + D)} \right) \right.$$
$$\left. \cdot \left(Z_m^* \, \xi_m^* \, a_m^* e^{j2\pi f(mT_s + \Delta_m)} + Z I_m^* \sum_{k=1}^{N_w - 1} \xi_{m,k}^* a_{m,k}^* e^{j2\pi f(mT_s + kT_r + c_{m,k}T_c + \theta_m T_B + \Delta_{m,k} + D)} \right) \right] \quad (7)$$

$$\Phi_{v_{BDM}}(f) = \frac{|G(f)|^2}{T_s} \left[\left(\sigma_\xi^2 + \mu_\xi^2\right)\left(\sigma_z^2 + \mu_z^2\right) - \mu_\xi^2 \mu_z^2 \phi_\Delta^2(f) + Z^2 \mu_\xi^2 \phi_\Delta^2(f) \Lambda_1(f) \left(\sigma_i^2 + \mu_i^2 - \mu_i^2 \phi_\theta^2(f)\right) \right.$$
$$\left. + \frac{1}{T_s} \mu_\xi^2 \phi_\Delta^2(f) \left(\mu_z^2 + 2Z\mu_z \mu_i \Lambda_2(f) \phi_\theta(f) + Z^2 \mu_i^2 \Lambda_1(f) \phi_\theta^2(f)\right) \sum_{l=-\infty}^{+\infty} \delta(f - \frac{l}{T_s}) \right] \quad (10)$$

Because of the periodicity of the PRDS and PRTH codes and since $X_z >> X_a = X_c = T_s$, it should be noted that, $\phi_{ss}(n, n-m+k) = \phi_{ss}(n, n-m-k) = \phi_{ss}(n,k) = \phi_{ss}(k)$. Substituting Eqs. (8) and (9) into Eqs. (6) and (7) leads to a simplified relation for the average autocorrelation $\Phi_{v_{BDM}}(f)$ as (10), where $\Lambda_1(f) = \sum_{k=1}^{N_w-1} \sum_{k'=1}^{N_w-1} \phi_{ss}\left(k - k'\right) e^{-j2\pi f(k-k')T_r}$ and $\Lambda_2(f) = \sum_{k=1}^{N_w-1} \phi_{ss}(k) \cos\left(2\pi f\left(kT_r + D\right)\right)$.

Note that Eq. (10) indicates the coefficients of spectral lines (i.e. the discrete part of $\Phi_{v_{BDM}}(f)$) clearly may be influenced by sinusoidal expressions $\Lambda_1(f)$, $\Lambda_2(f)$. This makes spectral lines to appear in the form of spectral spikes and spectral nulls, alternatively. However, the fact that both of them act as limiting factors in maximization of the transmitted power spectrum under the FCC mask is obvious. Therefore, in this paper unlike the other mentioned references, we focus on the spectral-lines suppression instead of spectral spikes removal.

5.2 Correlated Data Stream

Accordingly, taking the squared magnitude of the Fourier transform of the $2T$-second observation of $v(t)$, based on the proposed signal model written for correlated data stream in (2), and then performing the statistical expectation gives

$$E\left[|V_N(f)|^2\right] = W_{I_{CBDM}} + W_{II_{CBDM}} \quad (11)$$

where the factor $W_{I_{CBDM}}$ accounts for the statistical expectation of the same indexed expressions and is evaluated as (12). To continue, let us define $Q\left(n, m, k, k', f\right) = E\left[G_{\sigma_{n,k}}(f) G^*_{\sigma_{m,k'}}(f)\right]$.

Also, under the stationary steady state assumption $P(\sigma_n = q_i) = P(g_{\sigma_n}(t) = g_{q_i}(t)) = P(G_{\sigma_n}(f) = G_{q_i}(f)) = \pi_i$stands for the signal selection probability at state q_i. In addition, P_{ij}^{γ} stands for the γ'th-step transition probability (that is the probability of being in state q_i and after γ transitions get to state q_j). Furthermore, when only a single pulse shape is used for both DSR and Data parts of UWB signals, we have $g_{\sigma_{n,k}}(t) = I_{\sigma_n} g\left(t - \theta_{\sigma_{n,k}} T_B\right)$, where T_B is the PPM modulation index. Also, I_{σ_n} and $\theta_{\sigma_{n,k}}$ are the kth correlated PAM and PPM variables used for the transmission of the nth data symbol so that, their values depend on the status of Moore-Markov model at time n. In this case, I_{σ_n} is generated by the data block as the input of Moore-Markov machine and $\theta_{\sigma_{n,k}}$ will be the output of Moore-Markov machine. Therefore, we have $G_{\sigma_{n,k}}(f) = I_{\sigma_n} G(f) e^{-j2\pi f \theta_{\sigma_{n,k}} T_B}$ and consequently $E\left[G_{\sigma_{n,k}}(f)\right] = E\left[G_{\sigma_{m,k'}}(f)\right] = G(f) R_{\sigma}(f)$ where $R_{\sigma}(f) = E\left[I_{\sigma_n} e^{-j2\pi f \theta_{\sigma_{n,k}} T_B}\right] = \sum_{i=0}^{N_M - 1} \pi_i I_{\sigma_i} e^{-j2\pi f \theta_{\sigma_{i,k}} T_B}$. Thus, after using simplification, $W_{I_{CBDM}}$ is formulated mathematically as (13).

Now, according to the property of a regular ergodic MC, the γ'th-step transition probabilities P_{ij}^{γ} converges to the steady-state probabilities π_i [11,19,20], i.e. $P_{ij}^{\gamma} \simeq \pi_j$, $P_{ji}^{\gamma} \simeq \pi_i$. Thus, the statistical expectation of the different indexed expressions, $W_{II_{CBDM}}$, can be written as Eq. (14). Substituting Eqs. (13), (14) in Eq. (11) and then substituting the result into Eq. (3), the average autocorrelation $\Phi_{v_{CBDM}}(f)$ is extracted after further mathematical manipulations, as (15).

$$
\begin{aligned}
W_{I_{CBDM}} = \sum_{n=-N}^{N} \Bigg[& E\left[Z_n Z_n^*\right] \left(\sigma_\xi^2 + \mu_\xi^2\right) |G(f)|^2 \\
& + 2Z.Re\left\{ E[Z_n^*] \sum_{k=1}^{N_w - 1} \mu_\xi^2 \phi_{ss}(n,k)\, \phi_\Delta^2(f) e^{-j2\pi f (kT_r + D)} E\left[G_{\sigma_{n,k}}(f)\right] G^*(f) \right\} \\
& + Z^2 \sum_{k=1}^{N_w - 1} \sum_{k'=1}^{N_w - 1} \mu_\xi^2 \phi_{ss}\left(n, k - k'\right) \phi_\Delta^2(f) e^{-j2\pi f (k-k') T_r} E\left[G_{\sigma_{n,k}}(f)\, G_{\sigma_{n,k'}}^*(f)\right] \Bigg]
\end{aligned} \tag{12}
$$

$$
\begin{aligned}
W_{I_{CBDM}} = (2N+1) \cdot \Big[& \left(\sigma_z^2 + \mu_z^2\right) \left(\sigma_\xi^2 + \mu_\xi^2\right) \\
& + 2Z\mu_z \sum_{k=1}^{N_w - 1} \mu_\xi^2 \phi_{ss}(k)\, \phi_\Delta^2(f) \left(\sum_{i=1}^{N_M - 1} \pi_i I_{\sigma_i} \cos 2\pi f \left(kT_r + \theta_{\sigma_{i,k}} T_B + D\right) \right) \\
& + Z^2 \mu_\xi^2 \sum_{k=1}^{N_w - 1} \sum_{k'=1}^{N_w - 1} \phi_{ss}\left(k - k'\right) \phi_\Delta^2(f) e^{-j2\pi f (k-k') T_r} \Big] \cdot |G(f)|^2
\end{aligned} \tag{13}
$$

$$
\begin{aligned}
W_{II_{CBDM}} = & \sum_{\substack{n=-N \\ m \neq n}}^{N} \sum_{m=-N}^{N} \mu_\xi^2 \phi_\Delta^2(f) \Bigg[\mu_z^2 + 2Z\mu_z \sum_{k=1}^{N_w - 1} \phi_{ss}(k) \left(\sum_{i=1}^{N_M - 1} \pi_i I_{\sigma_i} \cos 2\pi f \left(kT_r + \theta_{\sigma_{i,k}} T_B + D\right) \right) \\
& + Z^2 \sum_{k=1}^{N_w - 1} \sum_{k'=1}^{N_w - 1} \phi_{ss}\left(k - k'\right) Q_{\gamma \neq 0}(f)\, e^{-j2\pi f (k-k') T_r} \Bigg] \cdot |G(f)|^2 \cdot e^{-j2\pi f (n-m) T_s}
\end{aligned} \tag{14}
$$

$$
\begin{aligned}
\Phi_{v_{CBDM}}(f) = \frac{|G(f)|^2}{T_s} \Big[& \left(\sigma_\xi^2 + \mu_\xi^2\right) \left(\sigma_z^2 + \mu_z^2\right) - \mu_\xi^2 \mu_z^2 \phi_\Delta^2(f) + Z^2 \mu_\xi^2 \phi_\Delta^2(f) \Pi_1(f) \left(1 - Q_{\gamma \neq 0}(f)\right) \\
& + \frac{1}{T_s} \mu_\xi^2 \phi_\Delta^2(f) \left(\mu_z^2 + 2Z\mu_z \Pi_2(f) + Z^2 \Pi_1(f) Q_{\gamma \neq 0}(f)\right) \sum_{l=-\infty}^{+\infty} \delta\left(f - \frac{l}{T_s}\right) \Big]
\end{aligned} \tag{15}
$$

where $\Pi_1(f) = \sum_{k=1}^{N_w-1} \sum_{k'=1}^{N_w-1} \phi_{ss}(k-k')e^{-j2\pi f(k-k')T_r}$
$\Pi_2(f) = \sum_{k=1}^{N_w-1} \phi_{ss}(k) \sum_{i=1}^{N_M-1} \pi_i I_{\sigma_i} \cos 2\pi f \left(kT_r + \theta_{\sigma_{i,k}} T_B + D\right)$.

Comprehensive analysis of the average power spectral density presented for DSR-based UWB signals, results in clear investigations over other special cases. For example to achieve the PSD of DSR-based UWB signals with PAM (or PPM) as data modulation, simply drop the data parameter I_n (or θ_n). Clearly, ideal formulas can be obtained by ignoring timing jitter and attenuation factors. Meanwhile, Eq. (10) simply can be reduced to the PSD of conventional UWB signals [21] without DSR factor by cutting down the parameters associated to the DSR part and assuming $D = 0$.

6 SPECTRAL DESIGN STRATEGY

So far, ideal balanced and uncorrelated data streams have been assumed in many contributions and therefore undesired effects of the discrete part of spectrum (i.e. spectral lines) are not taken into account [13,14]. Furthermore, as discussed before, because of the synchronization problems the use of pseudo-random codes for spectrum shaping purposes cannot be justifiable. So, in this work, our idea is to find a convex optimization based method that can produce DSR-based signals using random process characteristics as the optimization variables. In fact, DSR signal gives us a degree of freedom to control undesired spectral lines, particularly in the case of non-symmetric data modulation schemes or unbalanced data sources. The first key factor that should be optimized is error function and is defined as,

$$e(f) = S_D(f) - \phi_v(f) \tag{16}$$

where, $S_D(f)$ is FCC or other standard spectral mask. Indeed, after the FCC definition, several emission limits have been defined by other governmental agencies around the world. In particular, the European standardization bodies (the European Telecommunications Standards Institute (ETSI), the European Committee for Electrotechnical Standardization (CENELEC), the Electronic Communications Committee (ECC), and the European Computer Manufacturers Association (ECMA)) are working jointly with governmental agencies with the purpose to define a new emission mask for UWB usage in Europe [5]. Anyway, the goal of the optimization is to minimize the error function so that the available power remains under a desired mask. This means that, in order to ensure that the power spectrum complies with the spectral standard, $e(f)$ must be positive for all frequencies. Another impressive factor that should be taken into account is $\eta(f)$ as the absolute ratio of the discrete part to the continuous part of the power spectrum $\phi_v(f)$ derived in section (5), over specific frequencies consisting of m/T_s, $m \in [L_1, L_2]$, where, L_1 and L_2 are lower and upper bounds of the desired range of frequencies under the mask, respectively. Note that $\eta(f)$ is not optimized in the continuous domain, but rather in the large enough number of discrete optimization points. Optimization points are uniformly distributed between L_1 and L_2. Furthermore, minimization of $\eta(f)$ is not done directly, but rather by the minimization of the difference between $S_D(f)$ and $\phi_v(f)$ i.e. $e(f)$. In order to advance the optimization problem, it is necessary to consider a set of samples taken from $\eta(f)$ and $e(f)$ over the discrete optimization points distributed over the mentioned frequency interval. To continue, let us define the following variables as,

$$\eta = \sum_{m=L_1}^{L_2} \eta(f)|_{f=\frac{m}{T_s}}, \ \varepsilon = \sum_{m=L_1}^{L_2} e_m \tag{17}$$

where $e_m = e(f)|_{f=\frac{m}{T_s}}$. Finally, in order to address all effective parameters, the related Cost Function (CF), as the spectral-lines strategy, based on nonlinear constraints is defined as,

$$\mu_z, \ \sigma_z : Min\ CF = \{\eta + \varepsilon\} \tag{18}$$

$$s.t.: \ e_m \geq 0, \ \forall m \in [L_1, L_2] \tag{19}$$

Each nonlinear constraint in Eq. (19) can be represented as a single constraint in the convex optimization toolbox. However, the defined problem is non-convex and accordingly cannot be regarded as a proper way for implementation in a convex program. Nevertheless, the appropriate form for the problem is rewritten as:

$$\mu_z, \ \sigma_z : Min\ CF = \left\{w_1\eta' + w_2\varepsilon'\right\} \tag{20}$$

subject to (19). where, $\eta' = \sum_{m=L_1}^{L_2} \eta^2(f)|_{f=\frac{m}{T_s}}$ and $\varepsilon' = \sum_{m=L_1}^{L_2} e_m^2$. Also, $\boldsymbol{W} = [w_1 \ w_2]$ is defined as the normalized weighting vector. Note that, the optimal point $\left(\mu_z, \sigma_z^2\right)$ cannot be acceptable unless it satisfies energy criterion over a transmitted symbol. This means that, over a transmitted symbol, for a conventional TR system, E_{Con}, the obtained energy for DSR signal, E_{DSR}, should not violate a predefined threshold, δ. Obtaining an acceptable optimal point $\left(\mu_z, \sigma_z^2\right)$, a sequence generator is exploited to produce the sequence $\{Z_n\}$ as DSR signal (Fig. 3). Note that the pulse magnitude, $|Z_n| = A$, offers a degree of freedom to address the generated sequence $\{Z_n\}$ in correspondence with optimal point $\left(\mu_z, \sigma_z^2\right)$.

7 PERFORMANCE EVALUATIONS

In this section, mathematical formulas for evaluation and maximization of the performance of the proposed DSR-based UWB system are derived. It is straightforward to write the energy equation as:

$$A^2 + (N_w - 1) Z^2 = \eta_\epsilon N_w \tag{21}$$

where $\eta_\epsilon = E_{DSR}/E_{Con.}$ and $\eta_\epsilon < \delta$. Signal $v(t)$ propagates through a multipath channel with impulse response $h_c(t) = \gamma \sum_{l=1}^{L} \alpha_l \delta(t - \tau_l)$ where $\delta(t)$ is the Dirac delta function, L is the number of resolvable multipath components, γ represents the shadowing, and α_l and τ_l respectively denote the amplitude and delay of the l'th multipath. After passing the multipath channel and the ideal pre-filter with impulse response $h_r(t)$, the

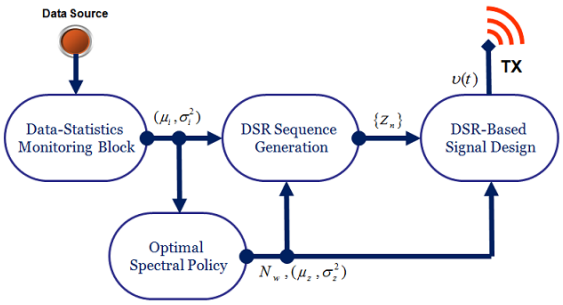

Fig. 3. Block diagram for the proposed DSR-based transmitter

$$r_f(t) = \gamma \left[A\xi_n g_r(t - nT_s - \Delta_n - \tau_s) + Z \sum_{k=1}^{N_w - 1} I_n \xi_{n,k} g_r(t - nT_s - kT_r - \theta_n T_B - \Delta_{n,k} - D - \tau_s) \right] + n(t) \tag{22}$$

$$\begin{aligned} H_{pq}^{ss} &= \int_0^{T_w} s(t)\, s(t + pT_r + \theta_q T_B + D)\, dt \\ &= \gamma^2 \sum_{k=1}^{N_w - 1} \int_0^{T_w} \xi_n \xi_{n,k} A Z I_n g_r(t - \Delta_n)\, g_r(t + (p-k)\, T_r + (\theta_q - \theta_n) T_B - \Delta_{n,k}) dt \end{aligned} \tag{25}$$

$$H_{pq}^{sn} = \int_0^{T_w} s(t)\, n(t + pT_r + \theta_q T_B + D)\, dt = \gamma \int_0^{T_w} \xi_n A g_r(t - \Delta_n)\, n(t + pT_r + \theta_q T_B + D) dt \tag{26}$$

$$\begin{aligned} H_{pq}^{ns} &= \int_0^{T_w} n(t)\, s(t + pT_r + \theta_q T_B + D)\, dt \\ &= \gamma \sum_{k=1}^{N_w - 1} \int_0^{T_w} \xi_{n,k} Z I_n n(t) g_r(t + (p-k)\, T_r + (\theta_q - \theta_n) T_B - \Delta_{n,k}) dt \end{aligned} \tag{27}$$

$$H_{pq}^{nn} = \int_0^{T_w} n(t)\, n(t + pT_r + \theta_q T_B + D)\, dt \tag{28}$$

received signal can be written as (22), where $\gamma g_r(t) = g(t) * h_c(t) * h_r(t)$, τ_s represents the time delay between the transmitter and the receiver, and $n(t)$ is the zero-mean Gaussian noise with a flat spectral density $N_0/2$ over the system bandwidth. Now, consider $r_f(t)$ as $r_f(t) = s(t) + n(t)$, where $s(t)$ is the received noise-free signal. Without loss of generality, we can assume that $\tau_s = 0$ to simplify the notations.

Assuming perfect timing and perfect estimates of channel coefficients and multipath delays, the correlator output of the p'th pulse according to the q'th possible pulse position is expressed as

$$H_{pq} = \int_0^{T_w} r_f(t)\, r_f(t + pT_r + \theta_q T_B + D) dt \tag{23}$$

where the length of the integration interval is assumed to be $T_w \simeq T_B$ in order to optimize the performance. We also assume that the product of noise bandwidth by integration interval $WT_w \gg 1$. Substituting Eq. (22) into Eq. (23) yields

$$H_{pq} = H_{pq}^{ss} + H_{pq}^{sn} + H_{pq}^{ns} + H_{pq}^{nn} \tag{24}$$

where, the parameters are defined as Eqs. (25-28).

According to (24), noise terms of the decision variable H_{pq} is defined as $N_{pq} = H_{pq} - H_{pq}^{ss}$. The variance of N_{pq} can be approximated, as (29).

$$\sigma_N^2 = E\left[N_{pq}^2\right] \simeq E\left[\left(H_{pq}^{sn}\right)^2\right] + E\left[\left(H_{pq}^{ns}\right)^2\right] + E\left[\left(H_{pq}^{nn}\right)^2\right] \tag{29}$$

Substituting Eqs. (31), (33) and (34) (See Appendix I) in Eq. (29) yield the following result

$$\sigma_N^2 = \gamma^2\left(\sigma_\xi^2 + \mu_\xi^2\right)\left(\frac{N_0}{2}\right)\left[A^2 E_I + Z^2\left(\sigma_i^2 + \mu_i^2\right)\sum_{k=1}^{N_w-1} E_{II}\right] + \frac{1}{2}N_0^2 T_w B \tag{35}$$

In continue, based on Eq. (25), the Inter-Symbol Interference (ISI) term can be expressed as

$$H_{pq}^{ISI} = \gamma^2 \sum_{\substack{k=1 \\ p\neq k}}^{N_w-1} \int_0^{T_w} \xi_n \xi_{n,k} AZ I_n g_r\left(t-\Delta_n\right) g_r(t+ (p-k)\,T_r + (\theta_q - \theta_n)T_B - \Delta_{n,k})dt \tag{36}$$

where $M_p^q = \int_0^{T_w} E\left[g_r\left(t-\Delta_n\right) g_r(t+pT_r+(\theta_q-\theta_n)T_B-\Delta_{n,k})\right]dt$, the mean and variance of the ISI term are respectively, derived as

$$\mu_{ISI} = E\left[H_{pq}^{ISI}\right] = \gamma^2\mu_\epsilon^2 AZ\mu_i \sum_{\substack{k=1 \\ p\neq k}}^{N_w-1} M_{p-k}^q \tag{37}$$

$$\sigma_{ISI}^2 = var\left(H_{pq}^{ISI}\right) = E\left[\left(H_{pq}^{ISI}\right)^2\right] - \mu_{ISI}^2 = \gamma^4 A^2 Z^2\left(\sigma_\xi^2 + 2\mu_\xi^2\right)\sigma_\xi^2\sigma_i^2 \sum_{\substack{k=1 \\ p\neq k}}^{N_w-1}\left(M_{p-k}^q\right)^2 \tag{38}$$

Considering Gaussian distribution for both ISI ($\sim \mathcal{N}(\mu_{ISI},\sigma_{ISI}^2)$) and noise ($\sim \mathcal{N}(0,\sigma_N^2)$), an upper bound for the probability of error for the p'th pulse in the DSR-based UWB system is then derived for a given channel realization, as follows:

$$P_e = E_\gamma\left[\left(\frac{M-2}{2}\right) erfc\left(\frac{\gamma^2\mu_\xi^2 AZM_0^n + \mu_{ISI}}{2\sqrt{\sigma_N^2+\sigma_{ISI}^2}}\right) + \frac{1}{2} erfc\left(\frac{\gamma^2\mu_\xi^2 AZM_0^n + \mu_{ISI}}{\sqrt{\sigma_N^2+\sigma_{ISI}^2}}\right)\right] \tag{39}$$

Now, the mean probability of error is then obtained by averaging over all pulses in the n'th symbol as

$$P_e^{DSR} = \frac{1}{N_w-1}\sum_{p=1}^{N_w-1} P_e = \frac{1}{N_w-1}\sum_{p=1}^{N_w-1} E_\gamma \left[\left(\frac{M-2}{2}\right) erfc\left(\frac{\gamma^2\mu_\xi^2 AZM_0^n + \mu_{ISI}}{2\sqrt{\sigma_N^2+\sigma_{ISI}^2}}\right) + \frac{1}{2} erfc\left(\frac{\gamma^2\mu_\xi^2 AZM_0^n + \mu_{ISI}}{\sqrt{\sigma_N^2+\sigma_{ISI}^2}}\right)\right] \tag{40}$$

Eventually, in order to achieve the optimal DSR-based UWB system, the optimum power allocation is determined according to the defined threshold, δ, which is designed for the energy criterion. To simplify the notation, we consider the probability of error of the first data pulse and minimize it over $|Z_n| = A$. Thus,

$$P_e^{DSR} \simeq \frac{1}{N_w-1}\sum_{p=1}^{N_w-1} E_\gamma\left[\left(\frac{M-2}{2}\right) erfc\left(\frac{\gamma^2\mu_\xi^2 AZM_0^n + \mu_{ISI}}{2\sqrt{\sigma_N^2+\sigma_{ISI}^2}}\right)_{p=1} + \frac{1}{2} erfc\left(\frac{\gamma^2\mu_\xi^2 AZM_0^n + \mu_{ISI}}{\sqrt{\sigma_N^2+\sigma_{ISI}^2}}\right)_{p=1}\right] \tag{41}$$

Substituting Eqs. (35), (37) and (38), the final form of Eq. (41) can be obtained. The above minimization is equivalent to maximizing Eq. (42) over $|Z_n| = A$. The last term in the both numerator and denominator of F can be neglected in high SNRs, as Eq. (43).

Substituting A^2 from the energy equation (21) with respect to Z^2 into Eq. (43) and setting its derivative with respect to Z^2, the optimal Z^* is simplified as

$$F = \frac{\left(\gamma^2\mu_\xi^2 AZM_0^n + \gamma^2\mu_\xi^2 AZ\mu_i \sum_{k=2}^{N_w-1} M_{1-k}^q\right)^2}{\gamma^2\left(\sigma_\xi^2+\mu_\xi^2\right)\left(\frac{N_0}{2}\right)\left[A^2E_I + Z^2\left(\sigma_i^2+\mu_i^2\right)\sum_{k=1}^{N_w-1}E_{II}\right] + \frac{1}{2}N_0^2T_wB + \gamma^4A^2Z^2(\sigma_\xi^2+2\mu_\xi^2)\sigma_\xi^2\sigma_i^2\sum_{k=2}^{N_w-1}\left(M_{1-k}^q\right)^2} \tag{42}$$

$$F \simeq \frac{\left(\gamma^2\mu_\xi^2 AZM_0^n\right)^2}{\gamma^2\left(\sigma_\xi^2+\mu_\xi^2\right)\left(\frac{N_0}{2}\right)\left[A^2E_I + Z^2\left(\sigma_i^2+\mu_i^2\right)\sum_{k=1}^{N_w-1}E_{II}\right] + \frac{1}{2}N_0^2T_wB} \tag{43}$$

$$Z^* = \sqrt{\frac{\eta_\epsilon N_w\left[\left(N_w-1\right)E_I - \sqrt{\left(N_w-1\right)\left(\sigma_i^2+\mu_i^2\right)E_I\sum_{k=1}^{N_w-1}E_{II}}\right]}{\left(N_w-1\right)^2E_I - \left(N_w-1\right)\left(\sigma_i^2+\mu_i^2\right)\sum_{k=1}^{N_w-1}E_{II}}} \tag{44}$$

8 OPTIMAL SPECTRAL POLICY

Here, an algorithmic approach is adopted in which the value of N_w is iteratively increased to reach an acceptable near-optimal point. The proposed optimization procedure can then be described in the following steps:

1. Set the initial value of N_w to two.
2. Estimate σ_i^2 and μ_i over the initial data frames for transmission.
3. Find Z^* to reach a reliable system over fading channels, based on Section (7).
4. Solve the optimization problem (20) to obtain σ_z^2 and μ_z. Here, we can design DSR-based system with DSR bits Z_n over the set $\{-A, +A\}$ according to optimal performance. This means that, when the optimization problem detects its acceptable optimal point $\left(\mu_z,\ \sigma_z^2\right)$, output symbol probabilities $p_{(Z_n=+A)}$ and $p_{(Z_n=-A)} = 1 - p_{(Z_n=+A)}$ must be estimated to produce DSR signal. Clearly, a same process can be performed over non-optimal values for $|Z_n| = A$ according to some predefined operational modes. However, in the case of performance-optimized signal model over fading channels, DSR generator should assign the optimal probability as: $p_{(Z_n=+A^*)}$: $Min\left\{\left(E\left[Z_n^*\right]-\mu_z\right)^2 + \left(E\left[\left(Z_n^*-\mu_z\right)^2\right]-\sigma_z^2\right)^2\right\}$.
5. Test the energy criterion: if $\eta_\epsilon < \delta$, go to step 8.
6. $N_w \leftarrow N_w + 1$.
7. Go to step 3.
8. End.

9 SIMULATION RESULTS

The objective of this section is twofold. Firstly, we investigate the spectral characteristics for the proposed spectral-efficient signal model and evaluate the system capability of spectral-lines suppression over different predefined operational modes; then, we take benefit of the accuracy of the analytical framework developed in this contribution to estimate the performance of DSR-based systems in multipath channels.

In the first set of results (Figs.5–7) here presented, the PSD plots and their corresponding spectral fluctuation ranges are obtained from Monte Carlo simulation for an independent or correlated unbalanced data stream that employs quaternary biorthogonal data modulation. Later, (Fig. 8), to illustrate the application of DSR-based transmission scheme, system performances are evaluated over IEEE CM1-2 802.15.3a channel models. All simulation results have been derived according to the same data source characteristics, enabling a straightforward comparison of the PSDs in the presence of a single narrow-band interferer with $f_c = 5.2GHz$ and SIR=$-15dB$. An unbalanced binary data source is assumed for all examples presented in this section. This source generates a sequence of independent or correlated binary symbols {0,1}, with respective probabilities $0 < p_0 < 1$ and $p_1 = 1 - p_0$. Indeed, alike practical systems, all the PSD plots presented in this section assume the following general signal parameters: $N_w = 5$; $T_r = 50ns$; $T_c = 3ns$; $T_p = 0.5ns$; $T_B = 1.5ns$; $D = 10ns$. It is also assumed that there is no pulse attenuation, and $\tau_d = 0.05ns$. Furthermore, we consider $T_g = 40ns$ as a "guard time" at the end of each data symbol.

Here, four scenarios are defined to evaluate the system performance as;

- Conventional TR system: Mode I
- Proposed DSR-based systems:
  Mode II:$[\eta_\epsilon = 1, |Z_n| = A = 1, Z = 1]$,

Mode III:$[\eta_\epsilon = 1, |Z_n| = A = 1.18, Z \simeq 0.89]$,
Mode IV:$[\eta_\epsilon = 1.2, |Z_n| = A = 1.13, Z \simeq 1]$.

Since the optimization process is carried out over the initial data frames, a traceable DSR sequence under the stationary data-stream assumption is rapidly computed. This means that the system complexity is not reflected as a major drawback. Here, we solve the optimization problem in (20) using gradient-based interior-point algorithm (See Fig. 4) where $\boldsymbol{W} = [0.908,\ 0.419]$.

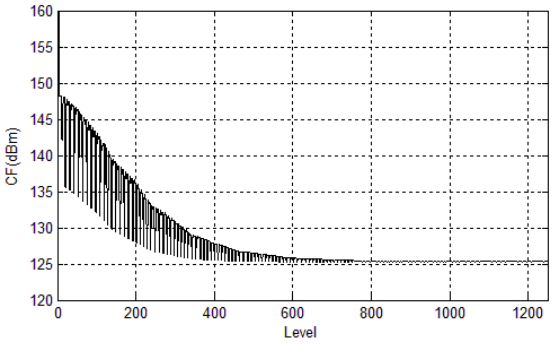

Fig. 4. The Cost Function (CF) minimization using the gradient-based interior-point algorithm

Figs. 5 and 6 represent PSD plots obtained for a stationary unbalanced binary data source with $p_0 = 0.35$ over the four different scenarios, respectively for uncorrelated and correlated data stream. Each figure compares the PSDs of both conventional and DSR-based systems. In order to run the optimization procedure, we assume $\delta = 1.3$. The sequences {0,1,3,2} [prime code over $GF(5)$] and {+1,-1,-1,+1,-1} are used for PR-TH and PR-DS as MA codes, respectively. In Fig. 5, the main spectral lines can be expected at intervals of $1/T_s$ for Mode I. Although this range for DSR-based UWB system turns out to be the same value, considerable spectral-lines suppression can be observed due to the deliberately inserted DSR signal. This means that the spectral lines vanish when DSR signal is employed, even when the data source produces non-uniform distributed symbols, i.e., when $p_0 \neq 0.5$. This is because of the balancing properties of the DSR signal as well-designed by Eq. (20). According to the results, the average fluctuation range (FR) of spectral lines for DSR-based system (Mode II) is $11.12dBm$ which indicates $17.14dBm$ decrement relative to the average FR for conventional TR system (Mode I). The results also show $18.70dBm$ and $20.10dBm$ decrements for Modes III and IV, respectively.

As expected before, because of the periodicity or unbalancing properties of the MC-modal considered in the case of correlated data stream as shown in Fig. 6, the process of spectral-line suppression becomes more complicated than the other independent data source. However, the obtained results are satisfactory and the value of average FR decreases from $36.17dBm$ in Conventional TR system (Mode I) to $26.36dBm$ in DSR-based UWB system (Mode III). Clearly, the penalty paid for spectral-lines suppression using DSR signal may be an excess power (i.e. when $\eta_\epsilon > 1$) which is spread throughout the power spectrum. However, a reasonable performance is achieved using a suitable predefined energy threshold, δ. Therefore the additional power spectrum (APS) is another essential factor in order to evaluate the DSR-based UWB system and is defined as can be observed in Fig. 7a. Next, to investigate the effect of the number of pulses used per transmitted symbol, N_w on the average FR and APS, Fig. 7b plots average FR and APS versus N_w for $A = 1,\ 2$ and PAM as data modulation. Indeed, a mixed case FR and APS analysis has been also considered in Fig. 7b, which reveals that the DSR-based spectral suppression still operates successfully even when there exists a power loss for the DSR pulses, as long as the number of pulses used per transmitted symbol, N_w, is well-assigned according to the energy criterion.

The spectrograms drown in Fig. 8, clearly indicate how the red color regions (i.e. high power frequencies due to undesired spectral lines) are strongly suppressed over the bandwidth in the case of DSR-based system. Simulation results also show that the average magnitude of $\eta(f)$, $e(f)$ respectively decreases from 25.7, $51.4dBm$ in conventional system to 3.1, $35.8dBm$ in DSR-based system for Mode IV (See Figs. 9 ,10).

The average probability of error (POE) for DSR-based system and conventional TR-modulated system over the two slow-faded CM1-2 channels is evaluated as Fig. 11. As shown by both analytical and simulation results, since the proposed scheme dedicates more power to the reference signal, a considerable performance improvement can be achieved. Fig. 11a shows that the DSR-based scheme represents about $1.8dB$, $3.1dB$ and $5.3dB$ performance improvement respectively for Modes II, III where ($\eta_\epsilon = 1$, i.e. no excess power needs to be injected into the system) and Mode IV, over the conventional TR-modulated scheme (Mode I) at $BER = 10^{-2}$. Clearly, slight performance degradation is expected in the case of correlated data stream (C. D. S.), as shown in Fig. 11b.

10 CONCLUSION

The presented framework is simple enough to enable a tractable analysis and can serve as a guideline for the design of rapid, efficient and reliable communication systems where coexistence between UWB and narrowband signals is of importance. Particular attention is devoted

to severely unbalanced (i.e. non-uniform distributed) data sources where a unified spectral analysis is considered for both uncorrelated and correlated M-ary biorthogonal data-stream scenarios. Indeed, the proposed DSR-based scheme as a modified version of TR-based signaling is presented in a way that optimized symmetric coefficients are applied to the consecutive reference signals in order to suppress undesired spectral-lines while self-synchronization properties of TR receiver are kept intact. Next, in order to achieve an optimal DSR-based UWB system, optimum power allocation is determined according to the defined threshold, δ, which is designed for the energy criterion. Both analytical and simulation results show that our system significantly outperforms the conventional TR-modulated system over the channel models CM1 and CM2.

REFERENCES

[1] Federal Communications Commission, "Revision of Part 15 of the Commissions Rules Regarding Ultra-Wideband Transmission Systems: First Report and Order," *Washington, DC*, ET-Docket 98-153, 2002.

[2] F. Nekoogar, "Ultra-Wideband Communications: Fundamentals and Applications," *Prentice Hall*, 2005.

[3] V. Sipal, B. Allen, D. Edwards and B. Honary, "Twenty years of ultra-wideband: Opportunities and challenges," *IET Communications*, Vol. 6, No. 10, pp. 1147-1162, July 2012.

[4] M. Chiani and A. Giorgetti, "Coexistence Between UWB and Narrow-Band Wireless Communication Systems," *Proceedings of the IEEE*, Vol. 97, No. 2, February 2009.

[5] G. Manzi, , M. Feliziani, P. A. Beeckman and N. V. Dijk, "Coexistence Between Ultra-Wideband Radio and Narrow-Band Wireless LAN Communication Systems Part I: Modeling and Measurement of UWB Radio Signals in Frequency and Time," *IEEE Trans. on Electromagnetic Compatibility*, Vol. 51, No. 2, May 2009.

[6] G. M. Maggio, N. Rulkov and L. Reggiani, "Pseudo-chaotic time hopping for UWB impulse radio," *IEEE Transactions on Circuits and Systems Part I*, vol. 48, No. 12, pp. 1424-1434, Dec. 2001.

[7] K. Kouassi, L. Clavier, I. Doumbia and P. Rolland, "Optimal PWR Codes for TH-PPM UWB Multiple-Access Interference Mitigation," *IEEE Communication Letters*, Vol. 17, No. 1, pp. 103-106, 2013.

[8] Y. P. Nakache and A. F. Molish, "Spectral shaping of UWB signals for time-hopping impulse radio," *IEEE J. on Selected Areas in Com.*, Vol. 24, No. 4, pp. 738-744, 2006.

[9] H. Nikookar and R. Prasad, "Introduction to Ultra Wideband for Wireless Communications," *Netherlands, Springer*, 2009.

[10] C. Wang, M. Ma, R. Ying and Y. Yang, "Narrowband Interference Mitigation in DS-UWB Systems," *IEEE Signal Processing Letters*, Vol. 17, No. 5, pp. 429-432, 2010.

[11] S. Villarreal-Reyes and R. M. Edwards, "Analysis Techniques for the Power Spectral Density Estimation of Convolutionally Coded Impulse Radio UWB Signals Subject to Attenuation and Timing Jitter," *IEEE Trans. on Veh. Tech.*, Vol. 58, No. 3, pp. 1355-1374, 2009.

[12] L. Reggiani and G. M. Maggio, "Coherent vs. non-coherent detection for orthogonal convolutional modulation: a trade-off analysis," *IEEE Int. Conf. on Ultra-wideband*, pp. 43-48, Sept. 2006.

[13] X. Wu, Z. Tian, T. N. Davidson and G. B. Giannakis, "Optimal waveform design for UWB radios," *IEEE Trans. on Signal Proc.*, Vol. 54, No. 6, 2009–2021, 2006.

[14] Y. Wang, X. Dong and I. J. Fair, "Spectrum Shaping and NBI Suppression in UWB Communications," *IEEE Trans. on Wireless Com.*, Vol. 6, No. 5, pp. 1944-1952, 2007.

[15] Z. Luo, H. Gao, Y. Liu and J. Gao, "A new UWB pulse design method for narrowband interference suppression," *IEEE Global Telecommun. Conf.*, pp. 388-392, Dec. 2004.

[16] G. D. Hingorani, and J. Hancock, "A Transmitted Reference System for Communication in Random or Unknown Channels," *IEEE Trans. on Commun.*, Vol. 13, No. 3, pp. 293-301, 1965.

[17] Y. L. Chao and R. A. Scholtz, "Ultra-Wideband Transmitted Reference Systems," *IEEE Trans on Veh. Tech.*, Vol. 54, No. 5, pp. 1556-1569, 2005.

[18] F. H. Panahi and A. Falahati, "Spectral efficient impulse radio-ultra-wideband transmission model in presence of pulse attenuation and timing jitter," *IET Communications*, Vol. 6, No. 11, pp. 1544-1554, 2012.

[19] J. R. Norris, "Markov Chains (Cambridge Series in Statistical and Probabilistic Mathematics)," *Cambridge University Press*, 1997.

[20] D. A. Levin, Y. Peres and E. L. Wilmer, "Markov Chains and Mixing Times," *American Mathematical Society*, 2008.

[21] J. G. Proakis, "Digital Communications," *New York: McGraw-Hill,* 1995.

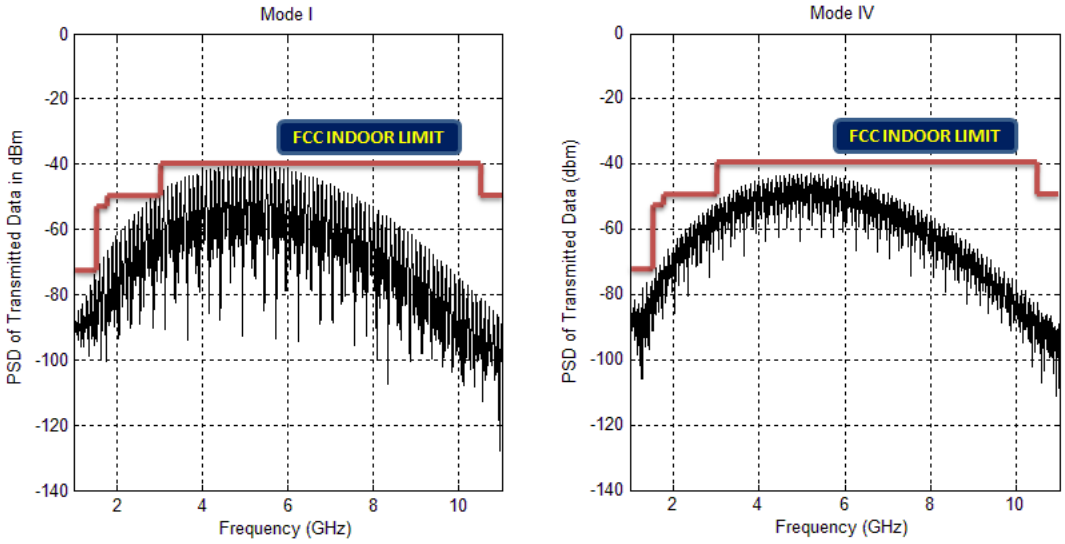

Fig. 5. PSD plot for quaternary biorthogonal data modulation over the defined modes I and IV.

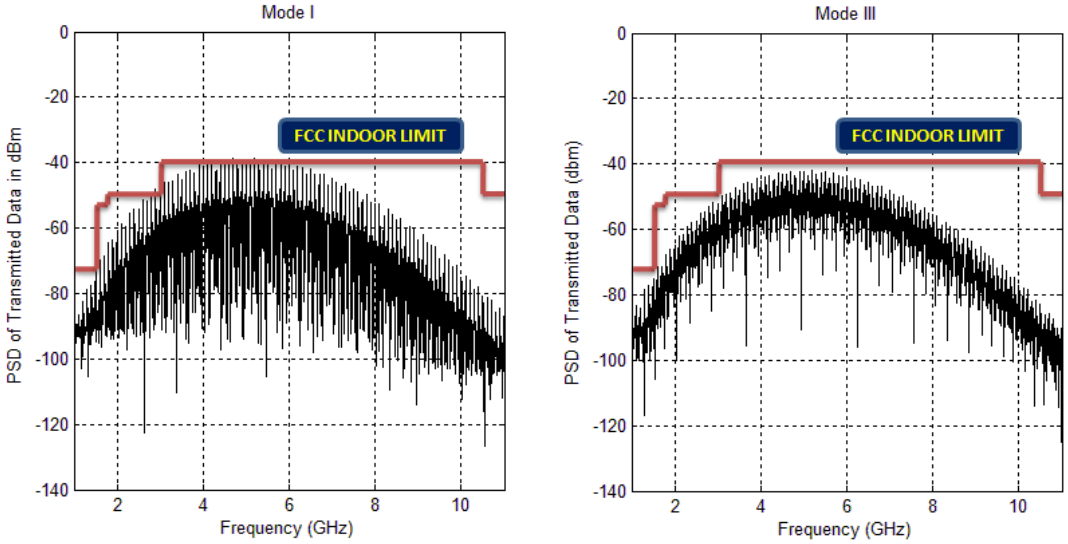

Fig. 6. PSD plot for correlated quaternary biorthogonal data modulation over the defined modes I and III.

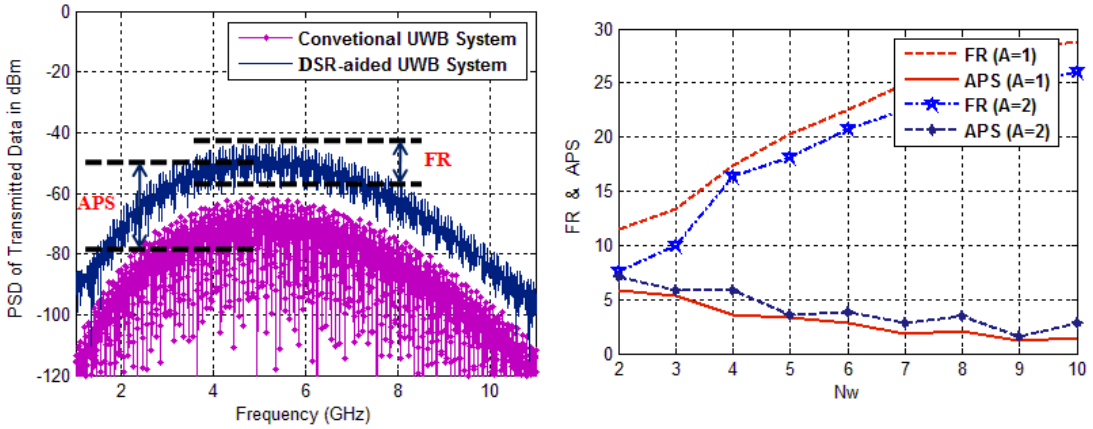

Fig. 7. (left) Essential factors in evaluation of DSR-based UWB system. (right) FR and APS versus N_w for $A = 1, 2$ and $Z = 1$.

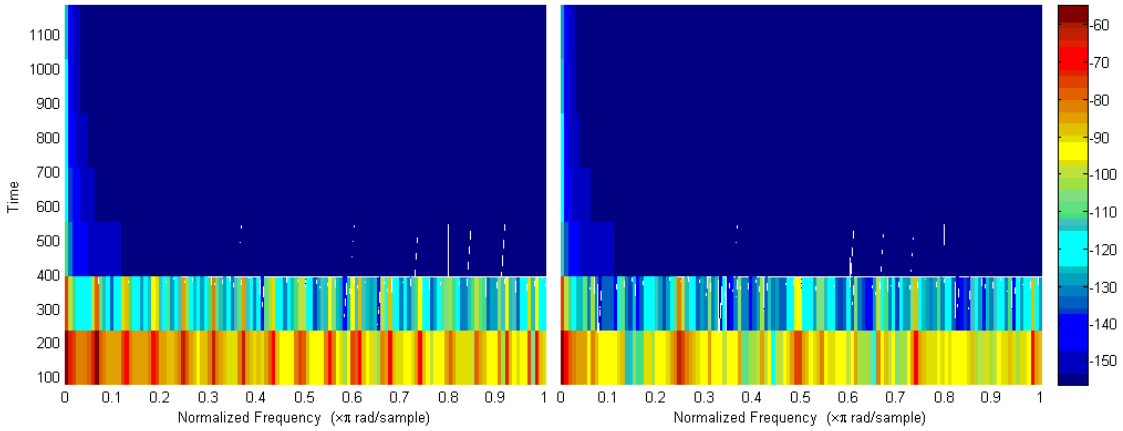

Fig. 8. Spectrograms for the PSD [dBm] of (left) Conventional TR system (right) DSR-based system

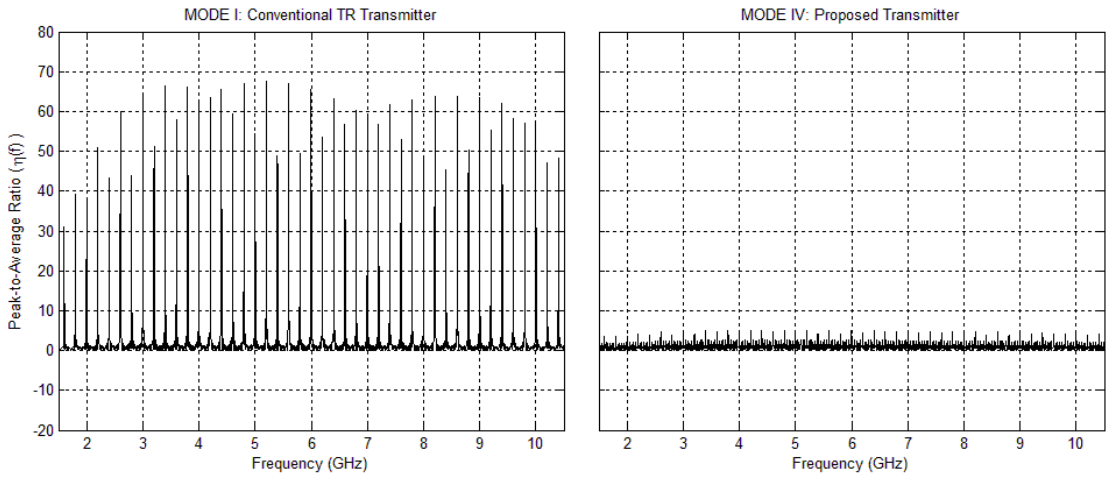

Fig. 9. The average magnitude of $\eta(f)$ for (left) Conventional TR system (right) DSR-based system

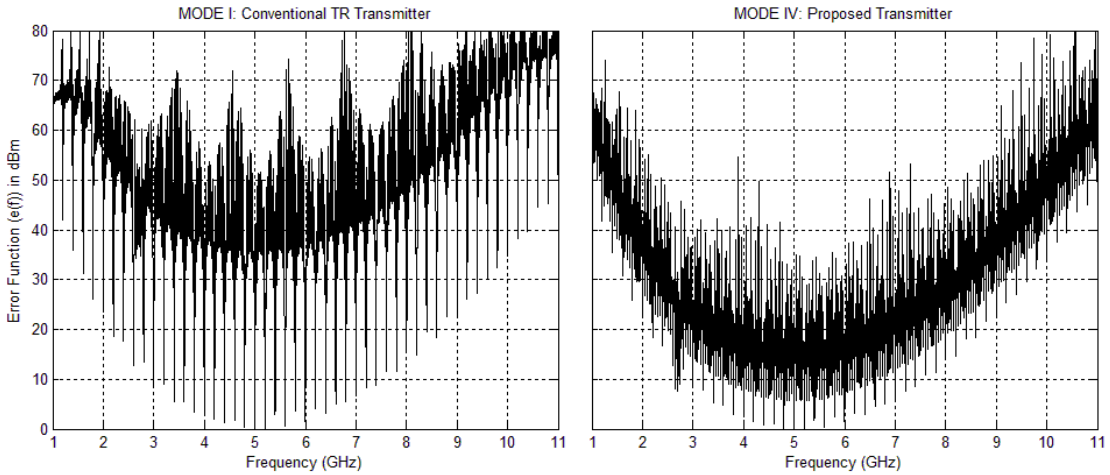

Fig. 10. The average magnitude of $e(f)$ for (left) Conventional TR system (right) DSR-based system

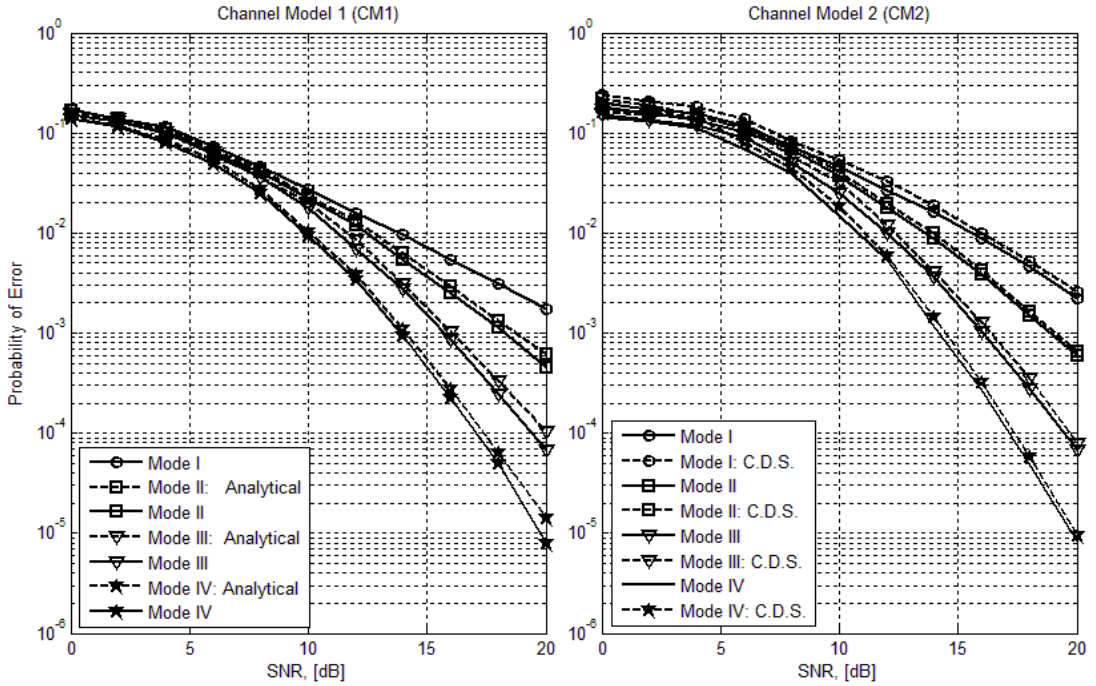

Fig. 11. POE versus SNR; Conventional TR system (Mode I) versus DSR-based systems (Mode II-IV) over the channel models CM1 (left) and CM2 (right)

APPENDIX I

$$E\left[\left(H_{pq}^{sn}\right)^2\right] = E\left[\gamma^2 \int_0^{T_w}\int_0^{T_w} \xi_n^2 A^2 g_r\left(t-\Delta_n\right) g_r\left(\tau-\Delta_n\right) n\left(t+pT_r+\theta_q T_B+D\right) n\left(\tau+pT_r+\theta_q T_B+D\right) dtd\tau\right]$$
$$= \gamma^2 A^2\left(\sigma_\xi^2+\mu_\xi^2\right)\int_0^{T_w}\int_0^{T_w} g_r\left(t-\Delta_n\right) g_r\left(\tau-\Delta_n\right)\varphi_n\left(t-\tau\right) dtd\tau$$
$$= \gamma^2 A^2\left(\sigma_\xi^2+\mu_\xi^2\right)\int_0^{T_w} g_r\left(t-\Delta_n\right)\int_{-\infty}^{+\infty} g_r\left(\tau-\Delta_n\right) U\left(T_w-\tau\right) U(\tau)\varphi_n\left(t-\tau\right) d\tau dt \tag{30}$$

where $\varphi_n(\tau)$, represents the autocorrelation function of $n(t)$ which is defined as $\varphi_n(\tau) = E[n(t+\tau)n(t)]$ with Fourier transform as $S_n(f)$. It is also defined $g_{u_I}(\tau)$ as $g_{u_I}(\tau) = g_r(\tau-\Delta_n)\,U(T_w-\tau)\,U(\tau)$, where $U(\tau)$ symbolizes the Unit Step Function. Hence

$$E\left[\left(H_{pq}^{sn}\right)^2\right] = \gamma^2 A^2\left(\sigma_\xi^2+\mu_\xi^2\right)\int_0^{T_w} g_r\left(t-\Delta_n\right)\int_{-\infty}^{+\infty} G_{u_I}(f)\, S_n(f)\, e^{j2\pi ft} df dt$$
$$\simeq \gamma^2 A^2\left(\sigma_\xi^2+\mu_\xi^2\right)\left(\frac{N_0}{2}\right)\int_0^{T_w} g_r\left(t-\Delta_n\right) g_{u_I}(t)\, dt = \gamma^2 A^2\left(\sigma_\xi^2+\mu_\xi^2\right)\left(\frac{N_0}{2}\right)\int_{-\infty}^{+\infty} g_{u_I}^2(t)\, dt$$
$$= \gamma^2 A^2\left(\sigma_\xi^2+\mu_\xi^2\right)\left(\frac{N_0}{2}\right) E_I \tag{31}$$

in which $E_I = \int_{-\infty}^{+\infty} g_{u_I}^2(t)\, dt$ denotes the energy of $g_{u_I}(t)$ with Fourier transform as $G_{u_I}(f)$, and

$$E\left[\left(H_{pq}^{ns}\right)^2\right] = \gamma^2\left(\sigma_\xi^2+\mu_\xi^2\right) Z^2\left(\sigma_i^2+\mu_i^2\right).$$
$$\cdot\int_0^{T_w}\sum_{k=1}^{N_w-1} E[g_r(t+(p-k)\,T_r+(\theta_q-\theta_n)T_B-\Delta_{n,k})\int_{-\infty}^{+\infty} g_{uII)I(}(\tau)\,\varphi_n(t-\tau)\,d\tau]\,dt \tag{32}$$

where $g_{u_{II}}(t)$ is defined as $g_{u_{II}}(t) = g_r\left(t+(p-k)T_r+(\theta_q-\theta_n)T_B-\Delta_{n,k}\right)U(T_w-t)\,U(t)$. Therefore Eq. (32) can be rewritten as

$$E\left[\left(H_{pq}^{ns}\right)^2\right] = \gamma^2\left(\sigma_\xi^2+\mu_\xi^2\right) Z^2\left(\sigma_i^2+\mu_i^2\right).$$
$$\cdot\int_0^{T_w}\sum_{k=1}^{N_w-1} E[g_r(t+(p-k)\,T_r+(\theta_q-\theta_n)T_B-\Delta_{n,k})\int_{-\infty}^{+\infty} G_{u_{II})I(}(f)S_n(f)\,e^{j2\pi ft}df]dt$$
$$\simeq \gamma^2\left(\sigma_\xi^2+\mu_\xi^2\right) Z^2\left(\sigma_i^2+\mu_i^2\right)\left(\frac{N_0}{2}\right)\sum_{k=1}^{N_w-1}\int_{-\infty}^{+\infty} E\left[g_{u_{II}}^2(t)\right] dt$$
$$= \gamma^2\left(\sigma_\xi^2+\mu_\xi^2\right) Z^2\left(\sigma_i^2+\mu_i^2\right)\left(\frac{N_0}{2}\right)\sum_{k=1}^{N_w-1} E_{II} \tag{33}$$

where $E_{II} = \int_{-\infty}^{+\infty} E\left[g_{u_{II}}^2(t)\right] dt$ denotes the energy of $g_{u_{II}}(t)$. Accordingly, the last term of Eq. (24) is simplified, as follows:

$$E\left[\left(H_{pq}^{nn}\right)^2\right] = \int_0^{T_w}\int_0^{T_w}\varphi_n^2(t-\tau)dtd\tau \le \int_0^{T_w}\int_{-\infty}^{+\infty}|S_n(f)|^2 df\, d\tau = \frac{1}{2}N_0^2 T_w B \tag{34}$$

F. H. Panahi received the B.S. in Electrical engineering from Tabriz University, Iran, in 2006 and also the M.S. and Ph.D. in Telecommunication engineering from the Iran University of Science and Technology (IUST), Tehran, in 2009 and 2015 respectively. He was the recipient of the University of Kurdistan (UoK) scholarship in 2010. Since 2015 he has been at University of Kurdistan (UoK) where he is presently an Assistant Professor in Information Theory, Channel Coding and Digital Communication Systems. His current research interests include green wireless communications, heterogeneous networks, Ultra-Wideband (UWB) and Cognitive Radio (CR) communications, and hardware implementations for digital technologies.

P. Farhadi received the B.S. degree in Information Technology (IT) Engineering from Azad University of Sanandaj, Iran, in 2012. Now, she is a Research Fellow at University of Kurdistan (UoK). Her current research interests include physical layer security, information technologies, heterogeneous computer networks, cognitive radio networks, and cooperative communications.

Z. H. Panahi received the B.S. (with high honors) and M.S., degrees in Plant Biotechnology Engineering from University of Kurdistan (UoK), Sanandaj, Iran, in 2010, and 2014, respectively. Her research interests has focused on the analysis of micro-biotechnology systems and biosensor networks based on green communication strategies and natural optimization algorithms.

AUTHORS' ADDRESSES

Farzad H. Panahi
Department of Electrical Engineering
Parvin Farhadi
Department of Information Technology (IT) Engineering
Zhila H. Panahi
Department of Plant Biotechnology Engineering
University of Kurdistan (UOK)
Iran, Kurdistan, Sanandaj, Pasdaran street.
email: f.hpanahi@uok.ac.ir, parvin.farhadi@gmail.com, zhila.h.panahi@gmail.com

Received: 2014-06-25
Accepted: 2015-03-05